



ELSEVIER

Available online at www.sciencedirect.com

ScienceDirect

Materials Today: Proceedings 00 (2014) 000–000

materialstoday:
PROCEEDINGSwww.materialstoday.com/proceedings

7th International Symposium On Macro- and Supramolecular Architectures and Materials

Metal and metal oxide transformation and texturing using pulsed fiber laser

**L. Kotsedi^{*1-2}, P. Sechogela¹⁻², S. M. Eaton³, A.G. Demir⁴
F. Franceschini⁴, B. Previtali⁴, R. Ramponi⁵, H.C. Swart⁶, M. Maaza¹⁻²**

¹UNESCO-UNISA Africa Chair in Nanosciences-Nanotechnology, College of Graduate Studies, University of South Africa, Muckleneuk ridge, PO Box 392, Pretoria-South Africa,

²Nanosciences African Network (NANOAFNET), iThemba LABS-National Research Foundation, 1 Old Faure road, Somerset West 7129, PO Box 722, Somerset West, Western Cape, South Africa.

³Physics Department, Politecnico di Milano, Piazza Leonardo Da Vinci, 32, 20133 Milano, Italy

⁴Department of Mechanical Engineering, Politecnico di Milano, Via La Masa 1, 20156 Bovisa, Italy

⁵IFN-CNR, Piazza Leonardo da Vinci, 23, 20133 Milano, Italy

⁶University of the Free State, Physics Department, 205 Nelson Mandela Drive, Park West, Bloemfontein, 9301

Abstract

Thin films of amorphous vanadium metal were deposited on a glass substrate using the electron beam evaporator, these thin films were then exposed to a focused 1064 nm wavelength nanosecond laser pulses. The laser fluence was selected such that it was below the ablation threshold of the films, x-ray diffraction measurement revealed the formation of an oxide phase of vanadium after the laser exposure. The time of flight-secondary ion mass spectrometry data analysis showed a uniform elemental distribution of the elements on the films, whereas the Rutherford backscattering spectrometry results showed that the concentration of oxygen as a function of the laser fluence was increasing, hinting to the incorporation of the oxygen atoms in the films as the laser fluence increases. UV-Vis-NIR percentage reflectance measurements showed small evolution in the visible part of the spectrum due to laser exposure.

© 2014 Elsevier Ltd. All rights reserved.

Selection and peer-review under responsibility of the Conference Committee Members of 7th International Symposium on Macro- and Supramolecular Architectures and Materials.

Keywords: Amorphous; Oxidation; High resolution SEM; Vanadium oxide; TOF-SIMS; UV-Vis-NIR reflectance; Laser fluence.

* Corresponding author. Tel.: +27218431145

E-mail address: Kotsedi@tlabs.ac.za

2214-7853 © 2014 Elsevier Ltd. All rights reserved.

Selection and peer-review under responsibility of the Conference Committee Members of 7th International Symposium on Macro- and Supramolecular Architectures and Materials.

1. Introduction

Amorphous metals and their alloys have been a subject of intense research in the field of materials science and engineering because of their peculiar physical properties compared to their crystalline counterpart. Amorphous materials can be characterized by their non-periodic atomic structure with a very short-range ordering when bonded to the nearest neighbor in an atomic matrix. They normally exhibit lower thermal conductivity and are mechanically stronger than the crystalline material [1-6], and also have the advantage of being able to possess large plastic deformation, since they do not have dislocations as a result of defects in the crystalline metal [7-10].

This class of material has found many applications in the automotive industries, electronics and medical sciences. Amorphous metals and alloys can be prepared using various deposition methods such as physical vapor deposition [11-13], chemical vapor deposition [14] and wet chemistry methods [15-16]. Using these deposition methods, amorphous transition metal oxides can be grown on a substrate of choice. The challenge in growing oxides of transition metal is the inability to control their oxygen concentration and the stoichiometry of the grown thin films. This difficulty is attributed to the multiple valences nature of the transition metals [17].

One of the many transition metal oxides that have generated interest in the field of material science is the vanadium oxide. This is a multi-valence material, which has polymorphic phases, and also has photochromic and electrochromic properties that have lot of potential for technological and industrial applications [18]. Each valence state of the vanadium oxide presents interesting physical and chemical properties that need further research to better understand the mechanisms that governs their properties.

Lykissa *et al* prepared thin films of amorphous vanadium oxide by bombarding target material with ionized particles [19], when they conducted a study of density of state of amorphous V_2O_5 . Thin films of amorphous vanadium oxide (V_2O_5) have also been prepared using alternative methods such as the atomic layer deposition technique, whereby vanadyl oxytriisopropoxide and water were used as precursors in the reaction chamber to grow thin films of the amorphous V_2O_5 , which were then annealed to 330°C to transform them to an orthorhombic crystalline structure [20].

Another study has been conducted whereby vanadium carboxylate was spin coated on a silica glass substrate and the films were then exposed to KrF laser irradiation ($\lambda = 248 \text{ nm}$). After laser exposure, the initially amorphous films revealed the formation of a crystalline phase within the amorphous matrix [21]. Amorphous vanadium films have also been employed as a cathode material in battery research and wire casting technologies [15]. Furthermore, there has been a study whereby vanadium plates were illuminated with a CO_2 laser, resulting in the formation of different oxide structures with varying laser power [22]. The amorphous vanadium oxides were also observed on the plate when the laser power was increased to 20 W. The laser oxidation of this plate occurred as a result of laser irradiation being carried out in ambient air without any need for oxygen exposure.

In this work thin films of amorphous vanadium were deposited on a glass substrate in order to study the effect of laser exposure on the film, and determine the resultant microstructure as a function of the laser fluence.

2. Experimental details

Thin films of amorphous vanadium metal were deposited from a vanadium metal using an electron gun evaporator. The evaporation chamber was pumped down to the base pressure of 1×10^{-7} mbar before the evaporation of the element. The vanadium target was then degassed before the films were finally deposited on a glass substrate. The thickness of the grown film was measured to be 140 nm using a thickness crystal monitor. The thin films were then exposed to an Yb-doped fiber laser (YLP-1/100/50/50, IPG), pulsing at 1064 nm, with a repetition rate of 20 kHz and a pulse duration of 100 ns. A scanner head was used for beam manipulation (Sunny TSH 8310), which was equipped with a 100 mm focal lens to produce a beam diameter of 39 μm at focal plane [23]. The laser focus was

scanned at a speed of 20 mm/s, ensuring that multiple laser spots overlapped within the laser volume during patterning. A multiscan writing geometry was adopted [24], with a 25 μm transverse spacing between adjacent lines to form a square patterned area of 1.5 cm \times 1.5 cm using average laser fluence between 7.12 J/cm² and 11.81 J/cm².

2. Results and discussion

The microstructures of the pristine film and the laser patterned samples were studied using the D8 Advanced Bruker θ -2 θ x-ray diffractometer which uses the copper K α_1 x-rays with wavelength of 0.154 nm. The step size of the detector during the measurement was 0.050 degrees and all the samples were measured at room temperature. The corresponding x-ray diffraction patterns of all the samples are shown in Figure 1. The as-deposited films exhibit an amorphous microstructure as characterized by the hump around $2\theta = 25^\circ$. These amorphous samples were then laser irradiated with varying laser fluences. From the x-ray diffraction pattern plots of the laser surface structured films, the microstructure of the film remained amorphous after laser exposure as shown by the hump centred around $2\theta = 25^\circ$ for all the samples. For the samples exposed to the 7.12 J/cm² to 11.81 J/cm², there is a diffraction kink observed at $2\theta = 65^\circ$, whereas for the laser fluence of 11.81 J/cm² the diffraction peak is observed at $2\theta = 38.5^\circ$. These two peaks are not indexed since they could not be assigned to a specific JCPDS card number with high level of confidence. A second peak would be needed to properly match the peak with the JCPDS card with a high level of confidence. When higher laser fluence were used for the irradiation, the vanadium coatings were ablated from the glass substrate, therefore the samples exposed to higher laser fluences could not be analysed.

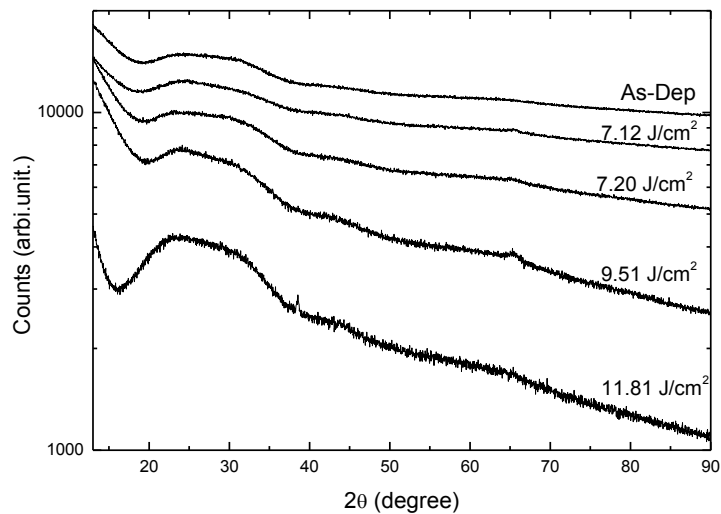


Figure 1: X-ray diffraction patterns of the as-deposited sample and the laser exposed samples.

This phenomenon of diffraction peaks that cannot be indexed from the JCPDS cards has also been reported in the work done by Fiedhouse *et al.* when they deposited the VO_x film using the DC sputtering method. Their films exhibited a crystallites of vanadium oxide embedded in the amorphous matrix as measured from the x-ray diffraction spectrometry [25].

M. Nishika *et al.* [21] also reported on a study where thin films amorphous vanadium were deposited on a glass substrate from a vanadium carboxylate precursor using spin coating technique. These films were then exposed to a UV laser with fluences ranging from 40 mJ/cm² to 80 mJ/cm² for 10 minutes, the film irradiated with a 40 mJ/cm² was still amorphous as observed from the x-ray diffraction patterns. It was only after the 80 mJ/cm² laser fluence

exposure that there was an emergence of a diffraction at $2\theta = 27.5^\circ$. The maximum temperature of the laser was calculated to be 1400°C using the one dimensional heat conduction equation. The resultant film after the laser exposure of 80 mJ/cm^2 was reported to have been crystallized, this was evident from a single diffraction peak, which was attributed to the VO_2 with the crystallites having a preferred orientation of (011), this indexing was assigned to the crystallites since the film was epitaxially grown on a substrate with a (011) orientation, it was not an indexing from a JCPDS file. From the interpretation of the x-ray diffraction pattern, it appears that these crystallites were embedded in an amorphous matrix, as it is the case in our study.

The Van de Graff accelerator was employed to determine the ratio of the vanadium-oxygen atoms in the samples using the Rutherford backscattering spectrometry. The specimen chamber was evacuated to 1×10^{-6} mbar before the samples were probed with the energetic 2.0 MeV He^{++} particles. The charge carried by the He^{++} beam was $20\text{ }\mu\text{C}$ and the detector angle was tilted to 170° relative to the sample holder. This was carried out to determine the stoichiometric ratio of the vanadium and oxygen atoms due to the laser irradiation in ambient air. RUMP software was used to simulate and fit the data extracted from the Rutherford backscattering spectrometry experimental measurements as shown in Figure 2. From the simulation data the stoichiometry of the vanadium and oxygen was varying as a function of the laser fluence. The as-deposited film from the RUMP simulation software has the V_5O_2 vanadium-oxygen ratio. Then the sample exposed to the laser fluence of 7.12 J/cm^2 has a stoichiometry of close to $\text{V}_{3.5}\text{O}_2$, and the samples exposed to the 7.20 J/cm^2 , 9.51 J/cm^2 and 11.81 J/cm^2 laser fluences, their stoichiometric was calculated to be, V_3O_2 , $\text{V}_{1.2}\text{O}_2$ and V_1O_2 respectively. The variation in stoichiometry as the laser fluence increases can be attributed to the non-isothermal and non-equilibrium dynamics of the laser heating during the laser exposure and the rapid heat dissipation on the sample due to the rapid temperature decrease which is in the nanosecond regime. The sample exposed to the 11.81 J/cm^2 of laser fluence has a similar stoichiometry to the sample exposed to the 80 mJ/cm^2 UV laser as observed from the work done by M. Nishikawa *et al.* were they used KrF laser with the wavelength of 248 nm to irradiate the samples [21].

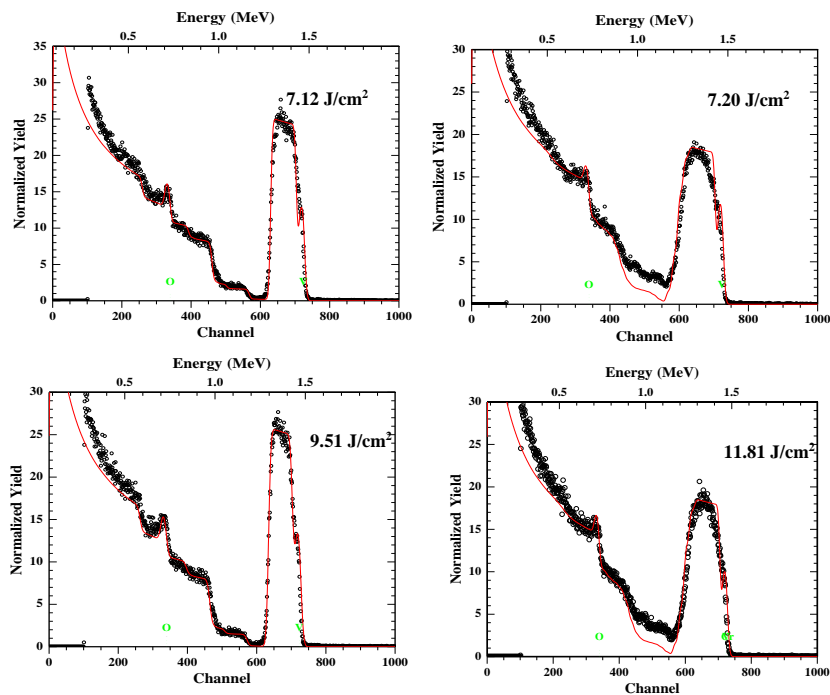


Figure 2: Rutherford backscattering spectrometry plots of the laser irradiated samples.

High resolution scanning electron microscopy was employed to study the morphology of the as-deposited sample and the laser exposed sample series. From Figure 3 (a-f) it is observed that the samples have developed cracks as a result of the laser exposure, with the density of the cracks increases with laser fluence. The observed cracks on the surface of the samples are attributed to the lattice shrinking of the vanadium film underneath the oxidized layer as a result of the strain introduced due to the laser heating. Similar cracks were observed when thin films of chromium on a glass substrate were exposed to the femtosecond laser in the work done L. Kotsedi et.al. [26]. Higher magnification micrographs in Figure 3 (e) taken on the crack show bubble like morphology formed on the cracks due to laser heating, which induces a melting process. In other studies reported on amorphous vanadium oxide [19], the laser exposed films showed crystallized grains of the films aggregated due to the low adhesion to the silica glass substrate because the interface between the film and substrate remained amorphous.

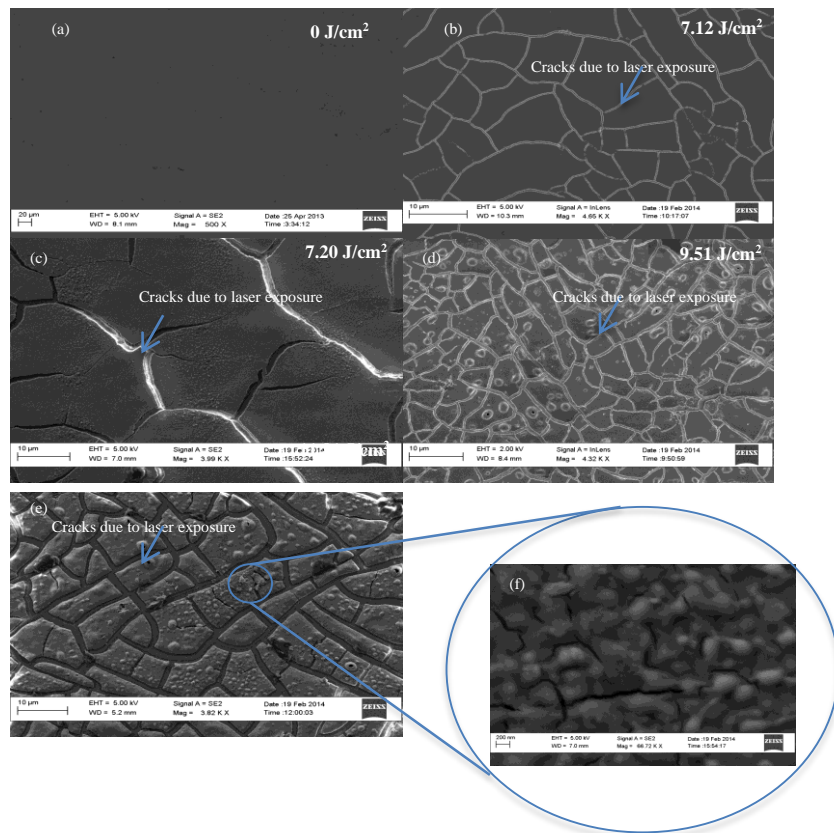


Figure 3 (a-f): High resolution electron microscope of the as-deposited and laser exposed vanadium thin films on glass substrate.

A representative measurement of elemental mapping of the samples was done using the IONTOF machine time of flight secondary ions mass spectrometry (TOF-SIMS) on the sample exposed to the laser fluence of 11.81 J/cm². This gave an elemental distribution image and the concentration of the elements after laser irradiation. The images of the thin film in positive polarity mode were acquired using a pulsed 30 kV Bi⁺ primary beam ion gun with a pulse repetition rate of 10 kHz. The spot size of the ion beam was 200 nm and the ion current was set at 0.25 pA. A bright pixel indicates a high intensity of the signal and the dark pixel indicates the low intensity. From Figures 4(a-j) there is a uniform distribution of vanadium and oxygen molecular ions (VO⁺) on the film surface. There is also a contribution of the VH⁺ molecular ions, which could be from the ionization of the water molecules from ambient air reacting with vanadium during the laser irradiation, this could not be detected using the Rutherford backscattering

spectrometry, since hydrogen atoms scatter at the energise well below the detection limit of the detecting electronics. The atomic ion Na^+ , Si^+ , K^+ and Ca^+ are from the glass substrate. The incorporation of the oxygen as measured from the TOF-SIMS corroborates the Rutherford backscattering spectrometry measurement where oxygen incorporation was also measured.

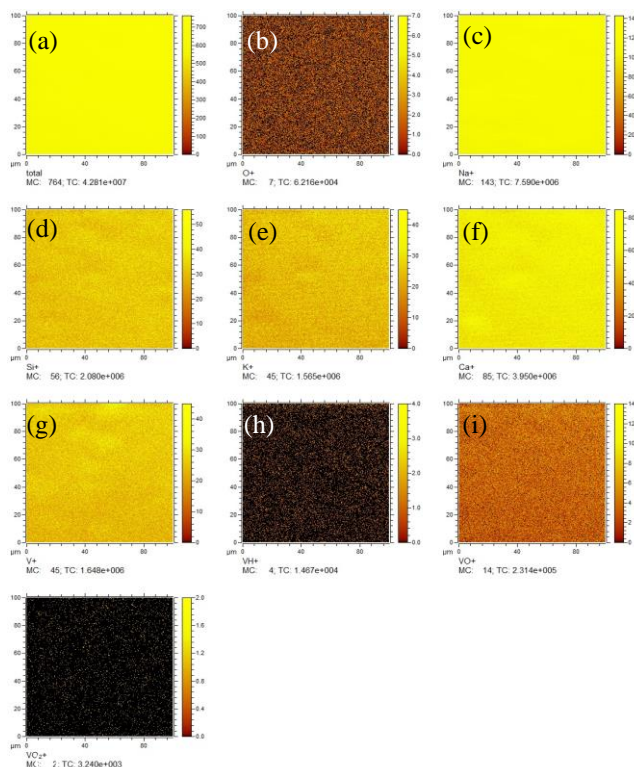


Fig 4 (a-j): TOF-SIMS micrographs of the sample exposed to 11.81 J/cm^2 of laser power in ambient air.

The UV-Vis-NIR spectroscopy responses of the sample exposed to laser radiation are shown in Figure 5 (a), and they exhibit a drop in percentage reflectance around 445 nm as compared to the as-deposited sample. This is due to the absorption of photons at that wavelength. This is evident from the colour change of the samples exposed to the laser irradiation as shown in Figure 5 (b). The samples exposed to the laser fluence of 7.12 J/cm^2 to 9.51 J/cm^2 show similar trends in the UV-Vis-NIR reflection spectroscopy, but for 11.81 J/cm^2 , a drop in reflectance begins at 380 nm with a further dip at 520 nm . This effect could be attributed to the crystallographic phase that was observed from the x-ray diffraction plot in Figure 1, of which samples exposed to lower laser fluences did not have.

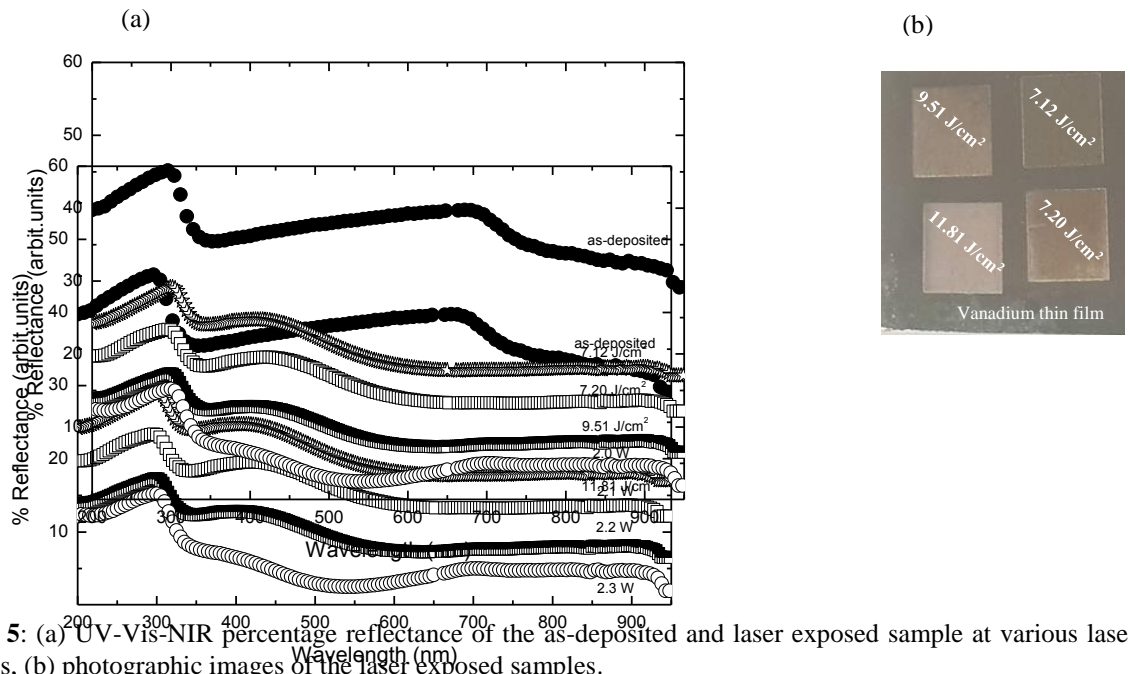


Figure 5: (a) UV-Vis-NIR percentage reflectance of the as-deposited and laser exposed sample at various laser fluences, (b) photographic images of the laser exposed samples.

4. Conclusions

Thin films of vanadium were deposited on a glass substrate from a vanadium metal target using electron beam evaporator. X-ray diffraction spectrometry was used to determine the microstructure of the films, from the x-ray plots, the as-deposited film was found to have an amorphous nature, whereas the laser irradiated samples were found to have amorphous nature, with small crystallites inclusion in the amorphous tissue due to the laser irradiation. The Rutherford backscattering spectrometry analysis of the samples showed an increase in oxygen content in relation to the increasing laser fluence with the stoichiometry of the sample exposed to the 11.81 J/cm² having a VO₂ vanadium to oxygen ratio. The elemental distribution of the 11.81 J/cm² laser irradiation showed that the distribution of the vanadium and oxygen atoms were uniform on the substrate as measured using TOF-SIMS spectrometry. The UV-Vis-NIR percentage reflectance of the laser irradiated samples showed a decrease reflectance in the visible region with photographic images revealing a change in colour of the samples due to laser irradiation.

5. Acknowledgements

The authors would like to express their gratitude to South African National Research Foundation under the grant number UID 92452.

6. References

- [1] T. Masumoto, R. Maddin, Mater. Sci. Eng. 19 (1975) 1-24.
- [2] H. Kimura, T. Masumoto, Scr. Mater. 9 (1975) 211-221.
- [3] J.J. Lewandowski, A.K. Thurston, P. Lowhaphandu, MRS Proceedings 754 (2002) CC9.3.

- [4] J.J. Lewandowski, M. Shazly, A. Shamimi Nouri, *Scr. Mater.* 54 (2006) 337–341.
- [5] M.F. Ashby, A.L. Greer, *Scr. Mater.* 54 (2006) 321–326.
- [6] M.F. Ashby, *Materials Selection in Mechanical Design*, second ed., Butterworth-Heinemann, Oxford, 1999.
- [7] J.H. Tregilgas, *Adv. Mater. Proc.* 162 (2004) 40.
- [8] M. Chen, A. Inoue, W. Zhang, T. Sakurai, *Phys. Rev. Lett.* 96 (2006) 245502.
- [9] D.C. Hofmann, G. Duan, W.L. Johnson, *Nature* 451 (2008) 1085–1089.
- [10] Y. Saotome, T. Hatori, T. Zhang, A. Inoue, *Intermetallics* 10 (2002), 1241–1247.
- [11] I.M. Ojovan, W. Lee, *J. Non-Cryst. Solids.* 356 (2010) 2534–2540.
- [12] A.J. Leenheer, J.D. Perkins, M.F.A.M. van Hest, J.J. Berry, R. P. O’Hayre, D.S. Ginley, *Phys. Rev. B* B77 (2008) 115215.
- [13] H. Yoshioka, Q. Yan, H. Habazaki, K. Asami, K. Hashimoto, *Corrosion Science.* 31 (1990) 349 – 354.
- [14] D.H. Kuo, B.Y. Cheung, R.J. Wu, *J-Non-Cryst Solids.* 324 (2003) 159 – 171.
- [15] H. Warlimont, *Mater. Sci. Eng. A* 304–306 (2001) 61–67.
- [16] S.S. Djokić, *J. Electrochem. Soc.* 146 (1999) 1824–1828.
- [17] A.D. Rata, A.R. Chezan, M.W. Haverkort, H.H. Hsieh, H.J. Lin, C.T. Chen, L.H. Tjeng T. Hibma, *Phys. Rev. B.* 69 (2004) 75404.
- [18] M.B. Sahana, M.S. Dharmaprasanth, S.A. Shivashankar, *J. Mater. Chem.* 12 (2002) 333-338.
- [19] I. Lykissa, S.-Y. Li, M. Ramzan, S. Chakraborty, R. Ahuja, C.G. Granqvist, G.A. Niklasson, *J. Appl. Phys.* 115 (2014) 183701.
- [20] X. Sun, C. Zhou, M. Xie, T. Hu, H. Sun, G. Xin, G. Wang. S.M. George, J. Lian, *Chem. Commun.* 50 (2014) 10703-10706.
- [21] M. Nishikawa, T. Nakajima, T. Manabe, T. Okutani, T. Tsuchiya, *JCS-Japan* 118 (2010) 788–791.
- [22] K. Sós, L. Nánai, A.M. Balint, *AIP Conference Proceedings* 1131 (2009) 102-105.
- [23] A. G. Demir, P. Maressa, B. Previtali, *Phys. Procedia* 41 (2013) 759-768.
- [24] S.M. Eaton, C. De Marco, R. Martinez-Vazquez, R. Ramponi, G. Cerullo, R. Osellame, *J. Biophotonics* 5 (2012) 687-702.
- [25] N. Fieldhouse, S.M. Pirsell, M.W. Horn, S.S. Bharadwaja, *J. Appl. Phys.* 42 (2009) 023707.
- [26] L. Kotsedi, Z.Y. Nuru, P. Mthunzi, T.F.G. Muller, S.M. Eaton, B. Julies, E. Manikandan, R. Ramponi, M. Maaza, *Appl. Surf. Sci.* 321 (2014) 560–565.